

Structures and Thermal Properties of Silver(I) (Poly)chalcogenide Halide Solid Solutions $\text{Ag}_{10}\text{Te}_{4-(q,p)}\text{Q}_{(q,p)}\text{Br}_3$ with $\text{Q} = \text{S, Se}$

Tom Nilges and Melanie Bawohl

Universität Münster, Institut für Anorganische und Analytische Chemie, Corrensstraße 30, 48149 Münster, Germany

Reprint requests to PD Dr. Tom Nilges. Fax: +49-251-83-36002. E-mail: nilges@uni-muenster.de

Z. Naturforsch. **2008**, *63b*, 629–636; received November 14, 2007

Dedicated to Professor Gérard Demazeau on the occasion of his 65th birthday

X-Ray diffraction experiments, thermal analyses and EDX spectroscopy were performed to determine the structural and thermal properties of the solid solutions $\text{Ag}_{10}\text{Te}_{4-q}\text{S}_q\text{Br}_3$ and $\text{Ag}_{10}\text{Te}_{4-p}\text{Se}_p\text{Br}_3$. The present investigation completes the work on silver(I) (poly)chalcogenide halides, a new class of mixed electron and ion conductors, with the general composition $\text{Ag}_{10}\text{Q}_4\text{X}_3$ ($\text{Q} = \text{chalcogen}$ and $\text{X} = \text{halogen}$). A high silver mobility within the polytelluride substructure and a pronounced polymorphism are characteristic features of these solid electrolytes. Phase transition temperatures are reduced upon the substitution of Te by the lighter homologs Se and S. Even low degrees of substitution lead to significantly lower phase transitions for the high-temperature polymorphs compared with $\text{Ag}_{10}\text{Te}_4\text{Br}_3$. A permanent disorder within the silver substructure is present for the maximally substituted sulfur containing phases.

Key words: Silver(I) (Poly)chalcogenide Halides, Ion Conductors, Thermal Analyses, Polymorphism

Introduction

The ternary system silver-chalcogen-halogen has been investigated for more than 30 years now. Compared with the copper- and gold-chalcogen-halogen systems the silver system is the one with the highest number of known ternary phases [1]. All ternary compounds are exclusively located on two different sections of the ternary phase diagram. AgIQ_3 ($\text{Q} = \text{Se, Te}$) [2, 3] and AgITe [4] are two members of the AgX -chalcogen section ($\text{X} = \text{halide}$) characterized exclusively by covalently bonded chalcogenide substructures. The remaining ternary compounds can be found on the quasi binary section AgX - Ag_2Q ($\text{Q} = \text{chalcogen}$). Ag_6TeBr_4 [5] was only postulated from electron diffraction experiments but could not be reproduced since then. A lot of interdisciplinary scientific work was spent on the characterization of Ag_3SX ($\text{X} = \text{Br, I}$) [6–8] due to the high silver ion conductivity. $\text{Ag}_5\text{Te}_2\text{Cl}$ [9–11] and substitution variants [12, 13] are silver ion conductors showing a large stability range indicating a partial anion exchange and an interesting sil-

ver ion mobility [14]. The same observation regarding the substitution variability was made for the Ag_3SX ($\text{X} = \text{Cl, Br, I}$) system [15, 16].

Recently, the first representative of a new class of silver ion conductors, $\text{Ag}_{10}\text{Te}_4\text{Br}_3$, was reported [1]. It represents the first member within the phase field AgX - Ag_2Q - Q featuring both isolated and covalently bonded chalcogen substructures. A structural frustration of the predominantly covalently bonded tellurium substructure and a pronounced polymorphism [17] are characteristic features of this compound. Four different polymorphs have been identified in the temperature range between 3 and 473 K with phase transition onset temperatures of $T_{\delta-\gamma} = 290$, $T_{\gamma-\beta} = 317$ and $T_{\beta-\alpha} = 355$ K, respectively. Partial substitution of bromide by other halides led to significant changes of these phase transition temperatures for the different polymorphs [18]. The partial exchange of Br by I led to a decrease of the transition temperatures while an increase was observed in the case of a partial Cl substitution.

The present work is dealing with the effects of a partial chalcogenide substitution on the structural and

thermal properties of $\text{Ag}_{10}\text{Te}_4\text{Br}_3$. X-Ray phase analyses, single crystal X-ray structure determinations and thermal analyses have been performed to delineate these effects.

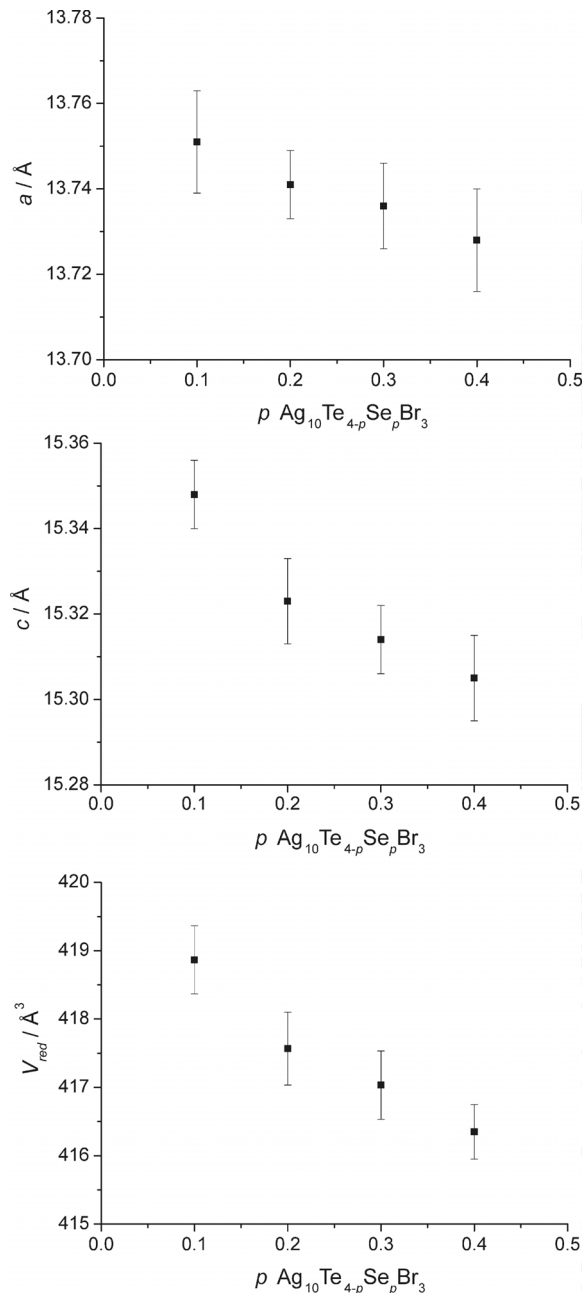


Fig. 1. Results of X-ray powder diffraction experiments for $\beta\text{-Ag}_{10}\text{Te}_{4-p}\text{Se}_p\text{Br}_3$ at 293 K. Error bars illustrate three times the standard deviation for the respective value. V_{red} represents the volume per formula unit.

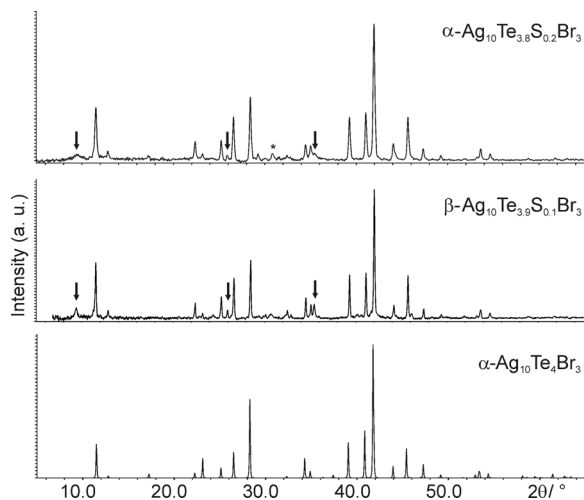


Fig. 2. X-Ray powder diffraction diagrams of the solid solution $\text{Ag}_{10}\text{Te}_{4-q}\text{S}_q\text{Br}_3$ with $q = 0-0.2$ at 293 K (data for $\alpha\text{-Ag}_{10}\text{Te}_4\text{Br}_3$; see ref. [17]). Characteristic reflections of the $\beta\text{-Ag}_{10}\text{Te}_4\text{Br}_3$ type realized for $\text{Ag}_{10}\text{Te}_{3.9}\text{S}_{0.1}\text{Br}_3$ are marked with an arrow. Contributions from both polymorphs are observed in the case of $\text{Ag}_{10}\text{Te}_{3.8}\text{S}_{0.2}\text{Br}_3$. The strongest reflection of a possible AgBr impurity is marked with an asterisk.

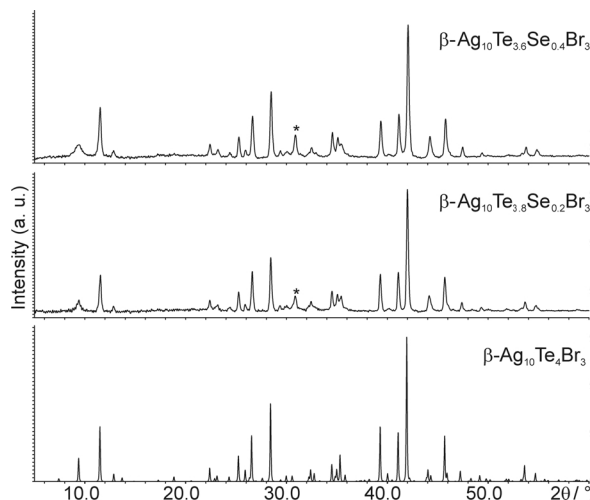


Fig. 3. X-Ray powder diffraction diagrams of the solid solution $\text{Ag}_{10}\text{Te}_{4-p}\text{Se}_p\text{Br}_3$ with $p = 0-0.4$ at 293 K (data for $\beta\text{-Ag}_{10}\text{Te}_4\text{Br}_3$; see ref. [17]). The strongest reflection of a possible AgBr impurity is marked with an asterisk.

Results and Discussion

Phase analytical X-ray powder diffraction analyses at 293 K proved a Vegard-like behavior [19] of the solid solution $\text{Ag}_{10}\text{Te}_{4-p}\text{Se}_p\text{Br}_3$ (Fig. 1).

The maximum degrees of substitution are $q = 0.2$ for $\text{Ag}_{10}\text{Te}_{4-q}\text{S}_q\text{Br}_3$ and $p = 0.4$ for $\text{Ag}_{10}\text{Te}_{4-p}\text{Se}_p\text{Br}_3$, re-

Compound	Composition	a , Å	c , Å	V , Å ³	Structure type
$\text{Ag}_{10}\text{Te}_{4-q}\text{S}_q\text{Br}_3$	q				
	0.1	13.752(4)	15.321(7)	2509.2(12)	β - $\text{Ag}_{10}\text{Te}_4\text{Br}_3$
	0.2	7.945(3)	7.669(4)	419.2(3)	α - $\text{Ag}_{10}\text{Te}_4\text{Br}_3$
$\text{Ag}_{10}\text{Te}_{4-p}\text{Se}_p\text{Br}_3$	p				
	0.1	13.751(6)	15.348(4)	2513.2(15)	β - $\text{Ag}_{10}\text{Te}_4\text{Br}_3$
	0.2	13.741(4)	15.323(5)	2505.4(16)	β - $\text{Ag}_{10}\text{Te}_4\text{Br}_3$
	0.3	13.737(7)	15.327(4)	2504.9(15)	β - $\text{Ag}_{10}\text{Te}_4\text{Br}_3$
	0.4	13.722(7)	15.305(5)	2498.1(12)	β - $\text{Ag}_{10}\text{Te}_4\text{Br}_3$

Table 1. Results from X-ray powder diffraction analyses of $\text{Ag}_{10}\text{Te}_{4-q}\text{S}_q\text{Br}_3$ and $\text{Ag}_{10}\text{Te}_{4-p}\text{Se}_p\text{Br}_3$ with $q = 0.1, 0.2$ and $p = 0.1-0.4$ at 293 K. Standard deviations are given in parentheses.

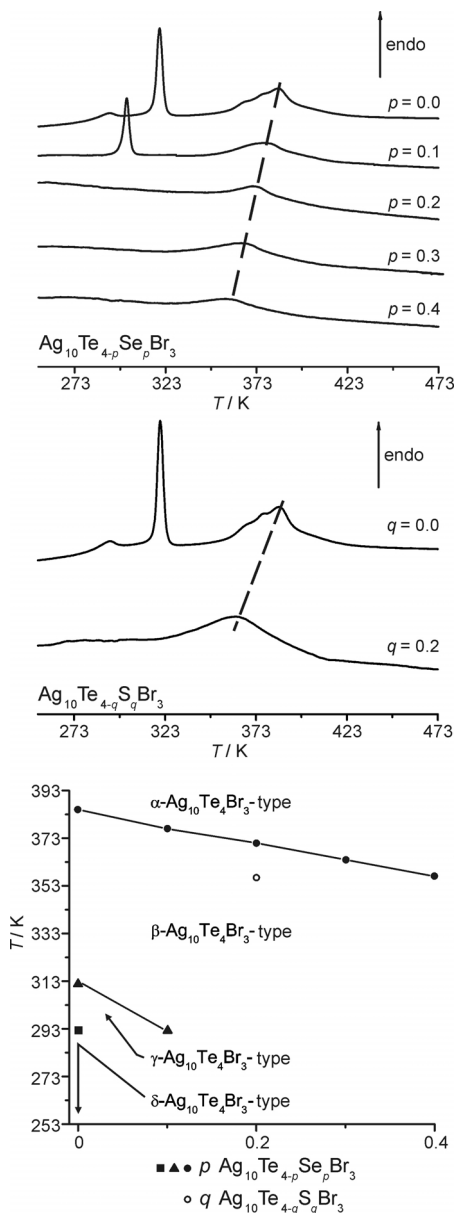


Fig. 4. Results of DSC measurements for $\text{Ag}_{10}\text{Te}_{4-p}\text{Se}_p\text{Br}_3$ and $\text{Ag}_{10}\text{Te}_{3.8}\text{S}_{0.2}\text{Br}_3$.

Table 2. Results from DSC measurements for $\text{Ag}_{10}\text{Te}_{3.8}\text{S}_{0.2}\text{Br}_3$ and $\text{Ag}_{10}\text{Te}_{4-p}\text{Se}_p\text{Br}_3$ with $p = 0-0.4$. $T_{\gamma-\beta}$ are onset values, $T_{\delta-\gamma}$ and $T_{\beta-\alpha}$ represent the maxima of the thermal effect. Measurements were performed in the temperature range between 113 and 473 K.

Compound	Composition	$T_{\delta-\gamma}$ / K	$T_{\gamma-\beta}$ / K	$T_{\beta-\alpha}$ / K
$\text{Ag}_{10}\text{Te}_4\text{Br}_3$	$q = p = 0$	290	317	385
$\text{Ag}_{10}\text{Te}_{4-q}\text{S}_q\text{Br}_3$	q			
	0.2	–	–	350
$\text{Ag}_{10}\text{Te}_{4-p}\text{Se}_p\text{Br}_3$	p			
	0.1	–	292	377
	0.2	–	–	371
	0.3	–	–	364
	0.4	–	–	357

spectively. All lattice parameters of the compounds are summarized in Table 1.

The lattice parameters and the observed powder patterns point towards the realization of the α - $\text{Ag}_{10}\text{Te}_4\text{Br}_3$ structure type for $\text{Ag}_{10}\text{Te}_{3.8}\text{S}_{0.2}\text{Br}_3$ and of the β - $\text{Ag}_{10}\text{Te}_4\text{Br}_3$ structure type for all selenium containing compounds and for $\text{Ag}_{10}\text{Te}_{3.9}\text{S}_{0.1}\text{Br}_3$ (Figs. 2 and 3). The powder diffractogram of $\text{Ag}_{10}\text{Te}_{3.8}\text{S}_{0.2}\text{Br}_3$ shows the characteristic reflections of the α -type but also some very broad and small reflections of the β -type (marked with arrows in Fig. 2). This finding can have two reasons: A small deviation in composition from crystal to crystal which often occurs in the case of solid solutions, or the close neighborhood of the phase transition temperature at r. t. in combination with a certain hysteresis of the transition itself.

The partial substitution within the anion substructure resulted in a continuous change in the structural and thermal properties of the solid solutions. Thermal analyses revealed a continuous decrease of the phase transition temperatures for the selenium containing samples up to the maximum degree of substitution of $p = 0.4$ in $\text{Ag}_{10}\text{Te}_{3.6}\text{Se}_{0.4}\text{Br}_3$ (Fig. 4).

The temperature of the β - α transition decreases continuously from 385 K for the ternary sample to 357 K for the maximally substituted selenium sample (see Table 2). Starting with $\text{Ag}_{10}\text{Te}_{3.8}\text{S}_{0.2}\text{Br}_3$ up

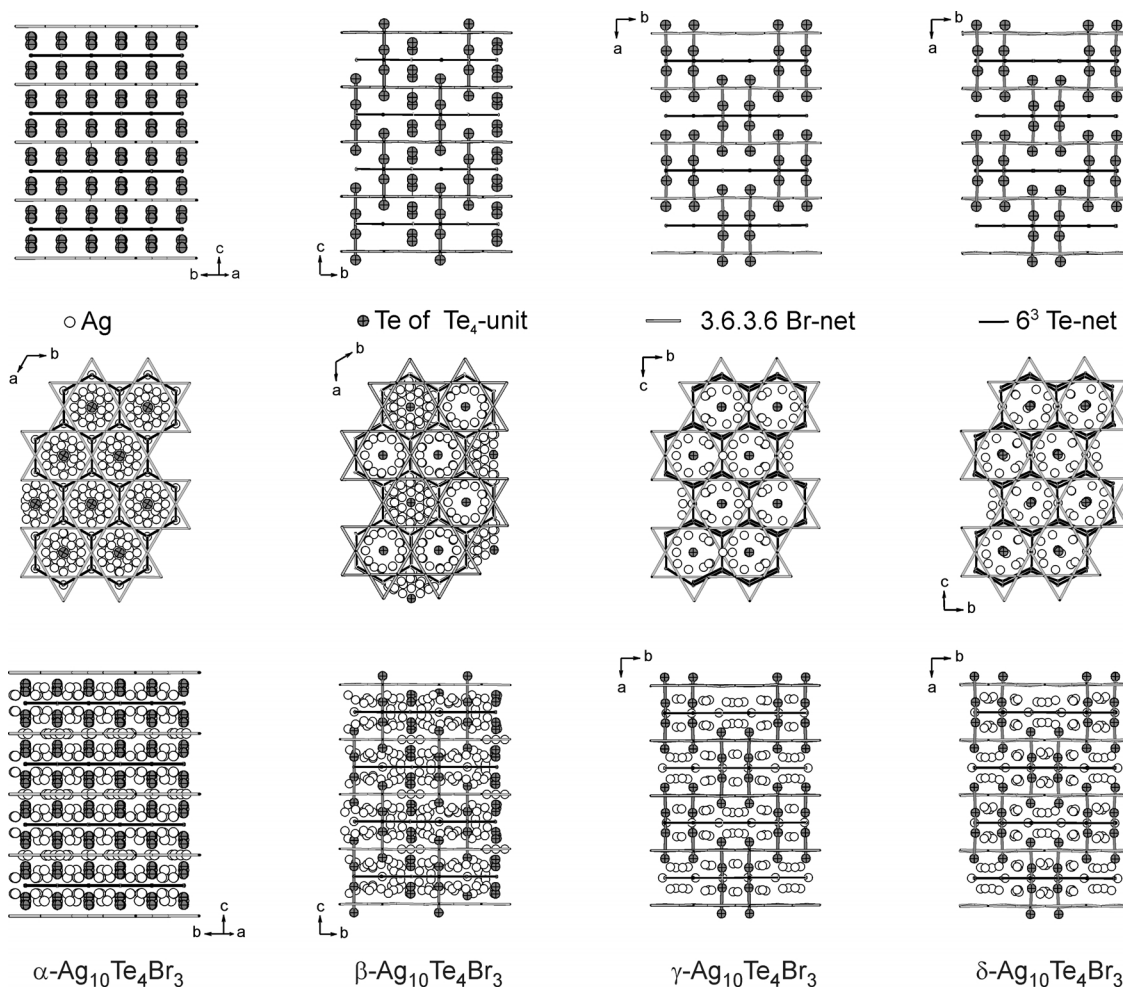


Fig. 5. Details of the $\text{Ag}_{10}\text{Te}_4\text{Br}_3$ structure types (data from ref. [17]). Top row: Anion substructure for the four existing polymorphs. The bromide and the non-covalently bonded tellurium substructure can be described by 3.6.3.6 and 6^3 nets applying a topological view without any bonding interaction between the positions. Middle and bottom row: Complete structure with disordered silver substructure for the α - and β - $\text{Ag}_{10}\text{Te}_4\text{Br}_3$ type and the ordered distribution for γ - and δ - $\text{Ag}_{10}\text{Te}_4\text{Br}_3$. The predominantly covalently bonded polytelluride substructure shows a partial (β -type) and a full (α -type) structural frustration leading to half occupied and closely neighbored Te-positions.

to the maximum degree of substitution no transition to the fully ordered γ -phase is observed. A comparable trend of the thermal properties is observed for the sulfur containing sample. The maximum degree of sulfur substitution is significantly lower ($q = 0.2$ in $\text{Ag}_{10}\text{Te}_{3.8}\text{S}_{0.2}\text{Br}_3$) compared with the selenium solid solution.

This finding is directly related to the ionic radii of the chalcogenide ions ($r(\text{S}^{2-}) = 1.70 \text{ \AA}$, $r(\text{Se}^{2-}) = 1.84 \text{ \AA}$ for CN = 6 [20]) substituting tellurium in the ternary compound. A chalcogen exchange with lighter homologs of tellurium is possible but only up to a

maximum of ten atom-% Se or five atom-% S. Obviously, the chalcogenide substitution can be used to stabilize the high-temperature polymorphs at lower temperatures. This procedure is well known for solid state electrolytes and is applied for example in the case of yttrium stabilized zirconia to achieve high oxygen conductivities at low temperatures [21, 22] for electrochemical applications [23–25]. The control of thermal and electrical properties can play a role for applications like non-volatile memory devices and atomic switches which require a good mixed conductor to create nano-sized dots for information storage [26]. Recent devel-

opments have shown that silver compounds like amorphous [27] or crystalline Ag_2S [28] are suitable for such applications.

Obviously the chalcogen substitution drastically changes the thermal properties, and the question arises whether the substitution has a significant effect on the structural features of the compounds. Two single crystal structure determinations have been performed for $\text{Ag}_{10}\text{Te}_{3.8}\text{S}_{0.2}\text{Br}_3$ and $\text{Ag}_{10}\text{Te}_{3.6}\text{Se}_{0.4}\text{Br}_3$ at 293 K, the maximally substituted phases, in order to substantiate the findings from phase analytical experiments, and to determine the realized polymorphs at that temperature. Fig. 5 illustrates the four existing polymorphs of the $\text{Ag}_{10}\text{Te}_4\text{Br}_3$ structure type [17]. A detailed structure description and discussion is reported for the ternary compound [1, 17], and only a short summary of characteristic features is given here (caption of Fig. 5).

Several problems, caused by the high degree of expected disorder and by the element combinations (Br/Se) for the present compounds (see Experimental Section for further details), appeared during the structure determination of the quaternary samples. Even after several homogenization and annealing steps and an optimization of the synthesis temperatures we were not able to prepare well scattering crystals to perform joint probability density function analyses. Nevertheless the quality was sufficient to collect data, and to determine the structures of the realized polymorphs. Some of the silver positions were described by a non harmonic approach due to the high silver mobility but no further discussion about structural parameters and compositions is appropriate due to the afore mentioned problems. The composition of the single crystals was confirmed by EDX measurements (see Table 5), and the quality of the structure determination was checked by a comparison of the calculated and measured powder diffractograms (Fig. 6).

Crystallographic data are summarized in Tables 3 and 4. Analyses of the determined structures substantiated the $\alpha\text{-Ag}_{10}\text{Te}_4\text{Br}_3$ structure type for $\text{Ag}_{10}\text{Te}_{3.8}\text{S}_{0.2}\text{Br}_3$ and the $\beta\text{-Ag}_{10}\text{Te}_4\text{Br}_3$ structure type for $\text{Ag}_{10}\text{Te}_{3.6}\text{Se}_{0.4}\text{Br}_3$ at 293 K. Both compounds are isostructural with the ternary polymorphs. Silver was completely disordered in both compounds, and a partial structural frustration of the covalently bonded tellurium substructure in $\text{Ag}_{10}\text{Te}_{3.6}\text{Se}_{0.4}\text{Br}_3$ and a complete frustration in $\text{Ag}_{10}\text{Te}_{3.8}\text{S}_{0.2}\text{Br}_3$ allow a reliable identification and classification of the polymorphs. In case of the sulfur substitution the high-temperature α -phase can be stabilized at r. t. which is in contrast to

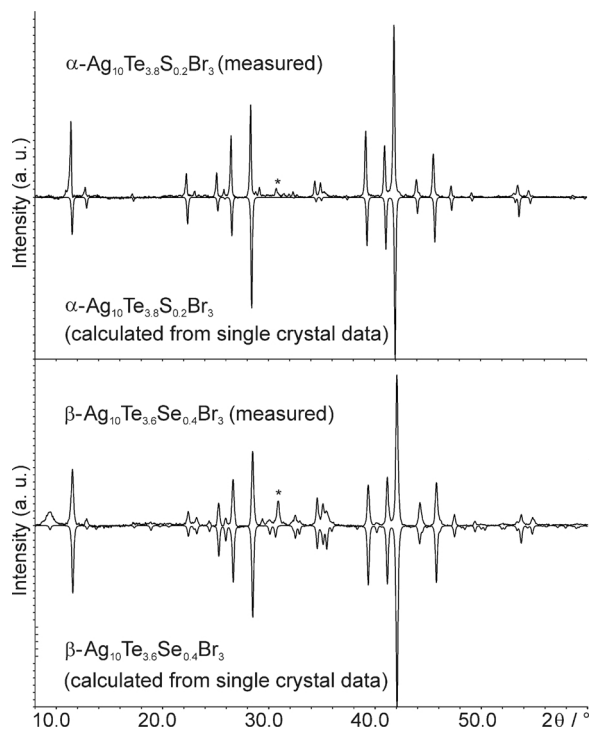


Fig. 6. Measured and calculated X-ray powder diffractograms of $\text{Ag}_{10}\text{Te}_{3.8}\text{S}_{0.2}\text{Br}_3$ and $\text{Ag}_{10}\text{Te}_{3.6}\text{Se}_{0.4}\text{Br}_3$ at 293 K. An AgBr impurity is marked with an asterisk.

the results of the thermal analysis but in agreement with the X-ray powder phase analysis. The broad β - α -phase transition in $\text{Ag}_{10}\text{Te}_{3.8}\text{S}_{0.2}\text{Br}_3$ lasts from 323 to 413 K while the structure determination was performed at 293 K just below the detected temperature range. Obviously the large difference in the chalcogenide radii results in a hysteresis of the phase transition which does not occur in the case of selenium substitution.

Conclusion

In the present study the structural and thermal properties of the solid solutions $\text{Ag}_{10}\text{Te}_{4-(q,p)}\text{Q}_{(q,p)}\text{Br}_3$ with $Q = \text{S}, \text{Se}$ were investigated. Thermal analyses proved the existence of phase transitions in good accordance with the non-substituted compound. Two structure determinations of the maximally substituted compounds substantiated the isostructural relation to the title compounds with the α - and β - $\text{Ag}_{10}\text{Te}_4\text{Br}_3$ structure type. The maximum degree of substitution was identified for both solid solutions. It differs significantly and is dependent on the chalcogen used. Five atom-% of tellurium can be replaced by sulfur,

Table 3. Selected crystallographic data for $\text{Ag}_{10}\text{Te}_{3.8}\text{S}_{0.2}\text{Br}_3$ and $\text{Ag}_{10}\text{Te}_{3.6}\text{Se}_{0.4}\text{Br}_3$ at 293 K.

Nominal composition	$\text{Ag}_{10}\text{Te}_{3.8}\text{S}_{0.2}\text{Br}_3$		$\text{Ag}_{10}\text{Te}_{3.6}\text{Se}_{0.4}\text{Br}_3$
Refined composition	$\text{Ag}_{10}\text{Te}_4\text{Br}_3$	$\text{Ag}_{10}\text{Te}_{3.92(9)}\text{S}_{0.08(9)}\text{Br}_3$	$\text{Ag}_{10.1(1)}\text{Te}_{3.6}\text{Se}_{0.4}\text{Br}_3$
Structure type	$\alpha\text{-Ag}_{10}\text{Te}_4\text{Br}_3$		$\beta\text{-Ag}_{10}\text{Te}_4\text{Br}_3$
Crystal size	$0.04 \times 0.03 \times 0.02$		$0.035 \times 0.025 \times 0.02$
Crystal system	hexagonal		hexagonal
Space group	$P6/mmm$ (no. 191)		$P6_3/mmc$ (no. 194)
a , Å	7.936(1)		13.722(7)
c , Å	7.684(1)		15.305(5)
V , Å ³	419.10(9)		2496(2)
Z	1		6
Diffractometer	IPDS II		IPDS II
Wavelength	Mo K_α radiation (0.71073 Å), graphite monochromator		
Total reflections	3630		9769
Independent reflections	247		1156
R_{int}	0.0586		0.3082
Refinement method	full-matrix least-squares on F^2 ; Gram-Charlier expansion, non harmonic refinement, program JANA 2000 [30]		
R ($I \geq 3\sigma I$)	0.0459	0.0439	0.0365
wR ($I \geq 3\sigma I$)	0.0718	0.0786	0.0440
R (all)	0.0770	0.0757	0.2692
wR (all)	0.0779	0.0866	0.0848
Parameter	43	48	163
Goof	2.19	2.21	1.65
Res. electron density max./min, e Å ⁻³	1.97/–1.57	2.03/–1.17	3.06/–2.69

Table 4. Atomic coordinates and isotropic displacement parameters for $\text{Ag}_{10}\text{Te}_{4-q}\text{S}_q\text{Br}_3$ with $q \approx 0.2$ refined without a sulfur content and for $\text{Ag}_{10}\text{Te}_{3.6}\text{Se}_{0.4}\text{Br}_3$ at 293 K.

	Wyckoff	sof	x	y	z	U_{iso}	
' $\text{Ag}_{10}\text{Te}_{4-q}\text{S}_q\text{Br}_3$ '	Te1_2a	2e	0.5	0	0	0.1801(5)	0.033(4)
	Te1_2b	2e	0.5	0	0	0.3085(11)	0.089(2)
	Te3	2d	1	2/3	1/3	1/2	0.083(3)
	Br1	3f	1	1/2	0	0	0.051(1)
	Ag1b	12p	0.081(4)	0.124(7)	0.211(5)	0	0.23(3)
	Ag3_7a	24r	0.165(4)	0.3922(16)	0.2033(12)	0.2544(11)	0.136(5)
	Ag3_7b	12n	0.330(7)	0	0.3035(17)	0.400(2)	0.196(7)
	Ag9	4h	0.28(3)	2/3	1/3	0.1916(13)	0.124(7)
	$\text{Ag}_{10}\text{Te}_{3.6}\text{Se}_{0.4}\text{Br}_3$	Te1	4f	0.9	2/3	1/3	0.4198(3)
Te2		4f	0.9	2/3	1/3	0.6593(4)	0.054(2)
Te3		12j	0.9	0.3428(4)	0.0089(3)	3/4	0.0561(19)
Se1		4f	0.1	2/3	1/3	0.4198	0.0343(16)
Se2		4f	0.1	2/3	1/3	0.6593	0.054(2)
Se3		12j	0.1	0.3428	0.0089	3/4	0.0561(19)
Br1		6g	1	1/2	0	1/2	0.046(4)
Br2		12k	1	0.3315(7)	0.1658(3)	0.4982(3)	0.050(2)
Te4a		4e	0.45	0	0	0.6556(8)	0.049(4)
Te4b		4e	0.45	0	0	0.5915(8)	0.021(3)
Se4a		4e	0.05	0	0	0.6556	0.049(4)
Se4b		4e	0.05	0	0	0.5915	0.021(3)
Ag1		2d	0.58(2)	2/3	1/3	1/4	0.035(4)
Ag1b		12i	0.207(13)	0.1122(14)	0	1/2	0.109(13)
Ag2		12k	0.31(2)	–0.0923(10)	–0.1845(19)	0.715(2)	0.155(15)
Ag2b		12k	0.56(3)	0.129(2)	–0.129(2)	0.686(4)	0.36(3)
Ag3		24l	0.486(16)	0.364(4)	–0.1291(15)	0.6400(12)	0.19(2)
Ag4		24l	0.521(18)	0.489(3)	0.1316(14)	0.6431(9)	0.265(14)
Ag5		12k	0.36(2)	0.2255(9)	–0.2255(9)	0.671(2)	0.086(16)
Ag7		12k	0.44(5)	0.451(2)	0.2255(10)	0.666(3)	0.24(3)
Ag8		24l	0.339(11)	–0.0212(19)	0.1817(15)	0.6267(13)	0.109(10)
Ag9	24l	0.193(8)	–0.025(4)	0.320(2)	0.5915(16)	0.27(2)	

Table 5. Results of EDX measurements (in atom-%) of the single crystals used for structure determinations. Results are averaged from 8 – 10 independent measurements at different points of the crystals. Standard deviations are estimated from the variations of the values.

Compound	Ag	Te	Se	S	Br
$\text{Ag}_{10}\text{Te}_{3.8}\text{S}_{0.2}\text{Br}_3$					
theoretical	58.8	22.4	–	1.2	17.6
measured	58(2)	20(2)		4(3)	18(2)
$\text{Ag}_{10}\text{Te}_{3.6}\text{Se}_{0.4}\text{Br}_3$					
theoretical	58.8	21.2	2.4		17.6
measured	60(2)	23(2)	2(2)	–	15(2)

and twice as much can be realized with selenium (10 atom-%). The difference in the degree of substitution is directly correlated with the size of the replacing ions. A significant lowering of the phase-transition temperatures occurs after substitution in both cases. In combination with the previously reported solid solutions $\text{Ag}_{10}\text{Te}_4\text{Br}_{3-x}\text{Cl}_x$ and $\text{Ag}_{10}\text{Te}_4\text{Br}_{3-y}\text{I}_y$, the present study reflects the large structural variability of the silver(I) (poly)chalcogenide halides. The variation of phase-transition temperatures, the mixed conductivity and the reasonable stability of the samples against humidity, light and oxygen is remarkable and may be interesting for industrial applications.

Experimental Section

Synthesis

The solid solutions $\text{Ag}_{10}\text{Te}_{4-q}\text{S}_q\text{Br}_3$ and $\text{Ag}_{10}\text{Te}_{4-p}\text{Se}_p\text{Br}_3$ were prepared by mixing silver (Chempur, 99.9%), tellurium (Chempur, 99.999%), selenium (Chempur, 99.999%), sulfur (Chempur, 99.999%) and silver(I) bromide (Chempur, 99+) in defined molar ratios according to the expected compositions. Starting from ternary $\text{Ag}_{10}\text{Te}_4\text{Br}_3$ the tellurium substructure was substituted by either sulfur or selenium in steps of $q, p = 0.1$ up to the maximum degrees of substitution. All starting materials were transferred to quartz ampoules, sealed at pressures lower than 10^{-3} mbar and heated up to 1223 K. The mixtures were quenched in an ice bath. After a homogenization step the mixtures were annealed at 613 K ($\text{Ag}_{10}\text{Te}_{4-p}\text{Se}_p\text{Br}_3$) and at 603 K ($\text{Ag}_{10}\text{Te}_{4-q}\text{S}_q\text{Br}_3$) for 10 to 14 d for each run. The homogenization and annealing process was repeated up to ten times in order to achieve phase purity of the samples. After each homogenization step the purity was checked by X-ray powder diffraction experiments. The compounds are light- and moisture-stable and can be stored and handled in air for several month.

Thermal analysis (DSC)

Thermal analyses (DSC) were performed using a Netzsch DSC 204t instrument under N_2 atmosphere in aluminum cru-

cibles. The temperature and enthalpy calibration was done at different temperatures using Hg, In, Sn, Bi, Zn and CsCl at a heating rate of 10 K/min. An accuracy of ± 1 K could be estimated from the calibration measurements for onset values. A temperature range of 113 to 473 K was applied to each sample under discussion. At least two consecutive runs were measured for each sample in order to check the reversibility of the observed effects. All results are derived from the second heating run for each sample. A standard deviation of ± 2 K was estimated for the derived values at the peak maxima due to the signal broadening at this position.

X-Ray powder and single crystal diffraction experiments

X-Ray powder diffraction phase analyses were performed to verify the phase purity and the maximal degrees of substitution for the solid solutions $\text{Ag}_{10}\text{Te}_{4-q}\text{S}_q\text{Br}_3$ and $\text{Ag}_{10}\text{Te}_{4-p}\text{Se}_p\text{Br}_3$. Finely ground samples were examined using a Stoe StadiP X-ray powder diffractometer operating with $\text{CuK}\alpha_1$ radiation ($\lambda = 1.54051 \text{ \AA}$) and equipped with a linear 5° position-sensitive detector (PSD, Braun). Silicon was used as an external standard. A comparison of measured and calculated powder diffractograms was performed for each of the existing polymorphs of the $\text{Ag}_{10}\text{Te}_4\text{Br}_3$ structure type (data from [17]).

Single crystals of suitable size were separated from the bulk materials of the nominal compositions $\text{Ag}_{10}\text{Te}_{3.8}\text{S}_{0.2}\text{Br}_3$ and $\text{Ag}_{10}\text{Te}_{3.6}\text{Se}_{0.4}\text{Br}_3$. Intensity data were collected on a Stoe IPDS II diffractometer, fitted with $\text{MoK}\alpha$ radiation ($\lambda = 0.71073 \text{ \AA}$). All data sets were corrected for Lorentz and polarization effects, and a numerical absorption correction was applied prior to the structure refinements. The numerical absorption correction for each data set was performed after an optimization of the crystal shape from symmetry equivalent reflections [29]. Structure models were derived from $\text{Ag}_{10}\text{Te}_4\text{Br}_3$ assuming an isostructural behavior of the substituted phases after the identification of the realized polymorph. It was not possible to refine [30] the silver distribution and the chalcogen contents simultaneously due to the high degree of disorder and the critical element combinations (for X-ray diffraction experiments) like Br/Se. Because of the pronounced substitutional disorder of the chalcogenide substructure and the obvious dynamic disorder within the cation structure several restraints were applied prior to the refinements.

For $\text{Ag}_{10}\text{Te}_{3.8}\text{S}_{0.2}\text{Br}_3$ a refinement of the chalcogen composition was not possible due to the low sulfur content. If sulfur and tellurium were introduced in the chalcogen positions the occupancy parameters did not show significant sulfur contents. Crystallographic data of the two refinements with and without a sulfur contribution are given for comparison in Table 3. Atomic coordinates are only presented for the refinement without a sulfur content in Table 4. Nevertheless,

the occurrence of the α -phase at 293 K clearly indicates the incorporation of sulfur into the sample. For pure $\text{Ag}_{10}\text{Te}_4\text{Br}_3$ the γ -phase can be observed at this temperature.

In the case of $\text{Ag}_{10}\text{Te}_{3.6}\text{Se}_{0.4}\text{Br}_3$ the chalcogen composition was set to the ideal value according to the starting composition. A free refinement of the chalcogen composition resulted in selenium contents higher than the maximum degree of substitution observed from phase analyses. Also the silver content dropped significantly below the ideal value of ten atoms per formula unit in this case. If the chalcogen composition was restricted to the ideal value a free refinement of the silver content resulted in ten atoms per formula unit within one times the standard deviation. Due to the limited quality of the data (reflected by the statistical parameters) especially for the selenium containing compound, we refrain from a discussion of the structural parameters in great detail. Notwithstanding, the data are in support of the conclusions drawn from the thermoanalytical and phase-analytical measurements of the realized polymorphs.

Further details of the crystal structure investigation may be obtained from Fachinformationszentrum Karlsruhe, 76344 Eggenstein-Leopoldshafen, Germany (fax: +49-7247-

808-666; e-mail: crysdata@fiz-karlsruhe.de, http://www.fiz-informationsdienste.de/en/DB/icsd/depot_anforderung.html) on quoting the deposition numbers CSD-418780 ($\text{Ag}_{10}\text{Te}_{3.6}\text{Se}_{0.4}\text{Br}_3$) and CSD-418781 ($\text{Ag}_{10}\text{Te}_{3.8}\text{S}_{0.2}\text{Br}_3$).

EDX analyses

Semiquantitative analyses of the single crystals used for structure determinations were performed using a Leica 420i scanning electron microscope equipped with an energy dispersive detector (EDX, Oxford). Ag, HgTe, Se, FeS_2 and KBr were used as standards for calibration. A voltage of 20 kV was applied to the samples. Low amounts of sulfur and selenium were detected for the two single crystals used for structure determinations. The results are summarized in Table 5.

Acknowledgements

This work was financed by the DFG within the SFB 458 'Ionenbewegung in Materialien mit ungeordneten Strukturen'. The DSC measurements performed by W. Prösting are gratefully acknowledged.

-
- [1] S. Lange, T. Nilges, *Chem. Mater.* **2006**, *18*, 2538.
 [2] M. Wagener, H.-J. Deiseroth, B. Engelen, C. Reiner, S. T. Kong, *Z. Anorg. Allg. Chem.* **2004**, *630*, 1765.
 [3] H.-J. Deiseroth, M. Wagener, E. Neumann, *Eur. J. Inorg. Chem.* **2004**, *24*, 4755.
 [4] F. Schnieders, P. Böttcher, *Z. Kristallogr.* **1995**, *210*, 323.
 [5] St. Karbanov, Z. Bontschewa-Mladenowa, N. Aramov, *Monatsh. Chem.* **1972**, *103*, 1496.
 [6] B. Reuter, K. Hardel, *Naturwissenschaften* **1961**, *48*, 161.
 [7] B. Reuter, K. Hardel, *Z. Anorg. Allg. Chem.* **1965**, *340*, 168.
 [8] S. Hull, D. A. Keen, N. J. G. Gardner, W. Hayes, *J. Phys.: Condens. Matter* **2001**, *13*, 2295.
 [9] R. Blachnik, H. Dreisbach, *J. Solid State Chem.* **1985**, *60*, 115.
 [10] T. Doert, E. Rönsch, F. Schnieders, P. Böttcher, J. Sieler, *Z. Anorg. Allg. Chem.* **2000**, *626*, 89.
 [11] T. Nilges, S. Nilges, A. Pfitzner, T. Doert, P. Böttcher, *Chem. Mater.* **2004**, *16*, 806.
 [12] T. Nilges, C. Dreher, A. Hezinger, *Solid State Sci.* **2005**, *7*, 79.
 [13] T. Nilges, S. Lange, *Z. Anorg. Allg. Chem.* **2005**, *631*, 3002.
 [14] C. Brinkmann, S. Faske, M. Michael, T. Nilges, A. Heuer, H. Eckert, *Phys. Chem. Chem. Phys.* **2005**, *8*, 369.
 [15] R. B. Beeken, K. L. Menningen, *J. Appl. Phys.* **1989**, *66*, 5340.
 [16] R. B. Beeken, T. J. Wright, T. Sakuma, *J. Appl. Phys.* **1999**, *85*, 7635.
 [17] S. Lange, M. Bawohl, D. Wilmer, H.-W. Meyer, H.-D. Wiemhöfer, T. Nilges, *Chem. Mater.* **2007**, *19*, 1401.
 [18] T. Nilges, M. Bawohl, S. Lange, *Z. Naturforsch.* **2007**, *62b*, 955.
 [19] L. Vegard, *Z. Phys.* **1921**, *17*.
 [20] R. D. Shannon, *Acta Crystallogr.* **1976**, *A32*, 751.
 [21] H. H. Möbius, B. Rohland, Patent DD64497, **1968**.
 [22] W. A. Fischer, D. Janke, *Z. Phys. Chem.* **1970**, *69*, 11.
 [23] J. H. Shim, C.-C. Chao, H. Huang, F. B. Prinz, *Chem. Mater.* **2007**, *19*, 3850.
 [24] F. M. B. Marques, V. V. Kharton, E. N. Naumovich, A. L. Shaula, A. V. Kovalevsky, A. A. Yaremchenko, *Solid State Ion.* **2006**, *177*, 1697.
 [25] J. B. Goodenough, *Ann. Rev. Mater. Res.* **2003**, *33*, 91.
 [26] R. Waser, M. Aono, *Nature Mater.* **2007**, *6*, 833.
 [27] W. C. West, K. Sieradzki, B. Kardynal, M. N. Kozicki, *J. Electrochem. Soc.* **1998**, *145*, 2971.
 [28] K. Terabe, T. Hasegawa, T. Nakayama, M. Aono, *Nature* **2005**, *433*, 47.
 [29] X-RED, X-SHAPE (versions 1.31 and 2.07), Programs for Absorption correction, Stoe & Cie, Darmstadt (Germany) **2005**.
 [30] V. Petricek, M. Dusek, L. Palatinus, JANA 2000, The Crystallographic Computing System, Institute of Physics, Praha (Czech Republic) **2000**.